Proceedings of the 34th
Conference on Decision & Control
New Orleans, LA - December 1995

Active Contours for visual tracking: a geometric gradient based approach

A. Kumar, A. Yezzi, S. Kichenassamy, P. Olver and A. Tannenbaum

Department of Electrical and Computer Engineering
University of Minnesota
Minneapolis, MN 55455
arun@aem.umn.edu

Abstract

In this note, we analyze the geometric active contour models proposed in [5, 19] from a curve evolution point of view and propose some modifications based on gradient flows relative to certain new metrics. This leads to a novel snake paradigm in which the feature of interest may be considered to lie at the bottom of a potential well. Thus the snake is attracted very naturally and efficiently to the desired feature. Moreover, we consider some 3-D active surface models based on these ideas.

1 Introduction

Recently, a number of approaches have been proposed for the problem of snakes or active contours. The underlying principle in these works is based upon the utilization of deformable contours which conform to various object shapes and motions. Snakes have been used for edge and curve detection, segmentation, shape modelling, and visual tracking, see the recent book by Blake and Yuille [3].

In this note, we consider a method based on the elegant approaches of Caselles *et al.* [5] and Malladi *et al.* [19]. In these papers, a level set curve evolution method is presented to solve the problem. Our idea is simply to note that both these approaches are based on Euclidean curve shortening evolution which in turn defines the gradient direction in which the Euclidean perimeter is shrinking as fast as possible. (See Section 2.) We therefore modify the active contour models of [5, 19] by multiplying the Euclidean arc-length by a function tailored to the features of interest to which we want to flow, and then writing down the resulting *gradient evolution equations.* This leads to some new snake models which efficiently attract the given active contour to the features of interest (which basically lie at the bottom of a *potential well*).

2 Euclidean Curve Shortening

The motivation for the equations underlying active geometric contours comes from *Euclidean curve shortening.* Therefore, in this section we will review the relevant curve evolution theory in the plane $\mathbf{R}^2$.

Accordingly, for κ the curvature, and $\vec{\mathcal{N}}$ the inward unit normal, one considers families of plane curves evolving according to the *geometric heat equation*

$$\frac{\partial C}{\partial t} = \kappa \vec{\mathcal{N}}. \tag{1}$$

This equation has a number of properties which make it very useful in image processing, [1, 15, 16].

Indeed, (1) is the Euclidean curve shortening flow, in the sense that the Euclidean perimeter shrinks as quickly as possible when the curve evolves according to (1) [9, 10, 13]. Since, we will need a similar argument for the snake model we discuss in the next section, let us work out the details.

Let $C = C(p,t)$ be a smooth family of closed curves where t parametrizes the family and p the given curve, say $0 \le p \le 1$. (Note we assume that $C(0,t) = C(1,t)$ and similarly for the first derivatives.) Consider the length functional

$$L(t) := \int_0^1 \|\frac{\partial C}{\partial p}\| dp.$$

Then differentiating (taking the "first variation"), and using integration by parts, we see that

$$\begin{aligned} L'(t) &= \int_0^1 \frac{\langle \frac{\partial C}{\partial p}, \frac{\partial^2 C}{\partial p \partial t} \rangle}{\|\frac{\partial C}{\partial p}\|} dp \\ &= -\int_0^1 \langle \frac{\partial C}{\partial t}, \frac{1}{\|\frac{\partial C}{\partial p}\|} \frac{\partial}{\partial p} \left[\frac{\frac{\partial C}{\partial p}}{\|\frac{\partial C}{\partial p}\|} \right] \|\frac{\partial C}{\partial p}\| \rangle dp. \end{aligned}$$

(Note that we multiplied and divided by $\|\frac{\partial C}{\partial p}\|$ in the latter integral.) But noticing now that

$$\|\frac{\partial C}{\partial p}\| dp =: ds$$

is (Euclidean) arc-length, and using the definition of curvature, the last integral is

$$-\int_0^{L(t)} \langle \frac{\partial C}{\partial t}, \kappa \vec{\mathcal{N}} \rangle ds$$

0-7803-2685-7/95 $4.00 © 1995 IEEE

that is, we see

$$L'(t) = -\int_0^{L(t)} \langle \frac{\partial C}{\partial t}, \kappa \vec{\mathcal{N}} \rangle ds.$$

Thus the direction in which $L(t)$ is decreasing most rapidly is when

$$\frac{\partial C}{\partial t} = \kappa \vec{\mathcal{N}}.$$

Thus (1) is precisely a gradient flow.

3 Active Snake Model

In two remarkable papers, Caselles *et al.* [5] and Malladi *et al.* [19] propose a snake model based on the level set formulation of the Euclidean curve shortening equation. More precisely, their model is

$$\frac{\partial \Psi}{\partial t} = \phi(x,y)\|\nabla\Psi\|(\mathrm{div}(\frac{\nabla\Psi}{\|\nabla\Psi\|}) + \nu). \qquad (2)$$

Here the function $\phi(x,y)$ depends on the given image and is used as a "stopping term." For example, the term $\phi(x,y)$ may be chosen to be small near an edge, and so acts to stop the evolution when the contour gets close to an edge. In [5, 19], the term

$$\phi := \frac{1}{1 + \|\nabla G_\sigma * I\|^2} \qquad (3)$$

is chosen, where I is the (grey-scale) image and G_σ is a Gaussian (smoothing filter) filter. The function $\Psi(x,y,t)$ evolves in (2) according to the associated level set flow for planar curve evolution in the normal direction with speed a function of curvature which was introduced in the fundamental work of Osher-Sethian [23, 24, 26, 27, 28].

It is important to note that as we have seen above, the Euclidean curve shortening part of this evolution, namely

$$\frac{\partial \Psi}{\partial t} = \|\nabla\Psi\|\mathrm{div}(\frac{\nabla\Psi}{\|\nabla\Psi\|}) \qquad (4)$$

is derived as a gradient flow for shrinking the perimeter as quickly as possible. As is explained in [5], the constant *inflation term* ν is added in (2) in order to keep the evolution moving in the proper direction. Note that we are taking Ψ to be negative in the interior and positive in the exterior of the zero level set.

Remarks 1.

1. In [19], the inflationary constant is considered both with a positive sign (inward evolution) and with a negative sign (outward or expanding evolution). In the latter case, this can be referred to as expanding "balloons." For simplicity, unless stated otherwise explicitly, we will take $\nu \geq 0$ (inward evolutions) in what follows below.
2. Instead of using a Gaussian to smooth the image one may of course use the a nonlinear smoothing filter based on the curvature; see [2].

We would like to modify the model (2) in a manner suggested by the computation in Section 1. Namely, we will change the ordinary Euclidean arc-length function along a curve $C = (x(p), y(p))^T$ with parameter p given by

$$ds = (x_p^2 + y_p^2)^{1/2} dp$$

to

$$ds_\phi = (x_p^2 + y_p^2)^{1/2} \phi dp,$$

where $\phi(x,y)$ is a positive differentiable function. We now essentially repeat the computation made in Section 2, i.e., we want to compute the corresponding gradient flow for shortening length relative to the new metric ds_ϕ.

Accordingly set

$$L_\phi(t) := \int_0^1 \|\frac{\partial C}{\partial p}\| \phi dp.$$

Let

$$\vec{T} := \frac{\partial C}{\partial p} / \|\frac{\partial C}{\partial p}\|,$$

denote the unit tangent. Then taking the first variation of the modified length function L_ϕ, and using integration by parts just as above, we get that

$$L'_\phi(t) = \int_0^{L_\phi(t)} \langle \frac{\partial C}{\partial t}, \phi\kappa\vec{\mathcal{N}} + (\nabla\phi \cdot \vec{T})\vec{T} - \nabla\phi \rangle ds_\phi$$

which means that the direction in which the L_ϕ perimeter is shrinking as fast as possible is given by

$$\frac{\partial C}{\partial t} = \phi\kappa\vec{\mathcal{N}} + (\nabla\phi \cdot \vec{T})\vec{T} - \nabla\phi. \qquad (5)$$

This is precisely the gradient flow corresponding to the miminization of the length functional L_v. Since the tangential component of equation (5) may be dropped (see [8]), this may be simplified to

$$\frac{\partial C}{\partial t} = \phi\kappa\vec{\mathcal{N}} - \nabla\phi. \qquad (6)$$

The level set version of this is

$$\frac{\partial \Psi}{\partial t} = \phi\|\nabla\Psi\|\mathrm{div}(\frac{\nabla\Psi}{\|\nabla\Psi\|}) - \nabla\phi \cdot \nabla\Psi. \qquad (7)$$

One expects that this evolution should attract the contour very quickly to the feature which lies at the bottom of the *potential well* described by the gradient

flow (7). As in [5, 19], we may also add a constant inflation term, and so derive a modified model of (2) given by

$$\frac{\partial \Psi}{\partial t} = \phi ||\nabla \Psi|| (\mathrm{div}(\frac{\nabla \Psi}{||\nabla \Psi||}) + \nu) - \nabla \phi \cdot \nabla \Psi. \quad (8)$$

Notice that for ϕ as in (3), $\nabla \phi$ will look like a doublet near an edge. Of course, one may choose other candidates for ϕ in order to pick out other features.

We have implemented this snake model based on the algorithms of Osher-Sethian [23, 24, 26, 27, 28] and Malladi *et al.* [19].

Remarks 2.

1. Note that the metric ds_ϕ has the property that it becomes small where ϕ is small and vice versa. Thus at such points lengths decrease and so one needs less "energy" in order to move. Consequently, it seems that such a metric is natural for attracting the deformable contour to an edge when ϕ has the form (3).

2. Kumar *et al.* [18] using a similar modification of the affine metric have developed an affine invariant snake model as well. In this case, the role of the function ϕ is played by an affine invariant edge detector developed in [18].

4 3-D Active Contour Models

In this section, we will discuss some possible geometric 3-D contour models based on surface evolution ideas, by modifying the Euclidean area in this case by a function which depends on the salient features which we wish to capture. In order to do this, we will need to set up some notation. (For all the relevant concepts on the differential geometry of surfaces, we refer the reader to [7].)

Let $S : [0,1] \times [0,1] \rightarrow \mathbf{R}^3$ denote a compact embedded surface with (local) coordinates (u, v). Let H denote the mean curvature and $\vec{\mathcal{N}}$ the inward unit normal. We set

$$S_u := \frac{\partial S}{\partial u}, \quad S_v := \frac{\partial S}{\partial v}.$$

Then the infinitesimal area on S is given by

$$dS = (||S_u||^2 ||S_v||^2 - \langle S_u, S_v \rangle^2)^{1/2} du dv.$$

Let $\phi : \Omega \rightarrow \mathbf{R}$ be a positive differentiable function defined on some open subset of $\mathbf{R}^3$. The function $\phi(x, y, z)$ will play the role of the "stopping" function ϕ given above in our snakes' model (7, 8).

It is a beautiful classical fact that the gradient flow associated to the area functional for surfaces (i.e., the direction in which area is shrinking most rapidly) is given by

$$\frac{\partial S}{\partial t} = H \vec{\mathcal{N}}. \quad (9)$$

(See [4, 11, 20, 22, 31] and the references therein.) What we propose to do is to replace the Euclidean area by a modified area depending on ϕ namely,

$$dS_\phi := \phi dS.$$

For a family of surfaces (with parameter t), consider the ϕ-area functional

$$A_\phi(t) := \int \int_S dS_\phi.$$

Once again, an integration by parts argument gives that

$$\frac{dA_\phi}{dt} = -\int \int_S \langle \frac{\partial S}{\partial t}, \phi H \vec{\mathcal{N}} - \nabla \phi + \text{tangential components} \rangle dS,$$

which after dropping the tangential part becomes

$$\frac{\partial S}{\partial t} = \phi H \vec{\mathcal{N}} - \nabla \phi. \quad (10)$$

The level set version of (10) is given in terms of $\Psi(x, y, z, t)$ by

$$\Psi_t = \phi ||\nabla \Psi|| \mathrm{div}(\frac{\nabla \Psi}{||\nabla \Psi||}) - \nabla \phi \cdot \nabla \Psi. \quad (11)$$

As before one may add a constant inflation term to the mean curvature to derive the model

$$\Psi_t = \phi ||\nabla \Psi|| (\mathrm{div}(\frac{\nabla \Psi}{||\nabla \Psi||}) + \nu) - \nabla \phi \cdot \nabla \Psi. \quad (12)$$

In the context of image processing, the term ϕ depends on the given 3-D image and is exactly analogous to the stopping term in (7, 8). It is important to note that there is a very big difference between the 2-D and 3-D models discussed here. Indeed, the geometric heat equation will shrink a simple closed curve to a round point, even if the curve is *nonconvex* without developing singularities. The geometric model (2) is based on this flow. For surfaces, it is well-known that singularities may develop in the mean curvature flow (9) of non-convex smooth surfaces [12]. (The classical example is the dumbbell.) We should note however that the mean curvature flow does indeed shrink smooth compact convex surfaces to round "spherical" points; see [14].

We should add that because of these problems, several researchers have proposed replacing mean curvature flow by flows which depend on the Gaussian curvature κ. Indeed, define

$$\kappa_+ := \max\{\kappa, 0\}.$$

Then Caselles and Sbert [6] have shown that the *affine invariant flow*

$$\frac{\partial S}{\partial t} = \text{sign}(H)\kappa_+^{1/4}\vec{\mathcal{N}} \tag{13}$$

will (smoothly) shrink rotationally symmetric compact surfaces to ellipsoidal shaped points. Thus one could replace the mean curvature part by $\text{sign}(H)\kappa_+^{1/4}$ in (12). Another possibility would be to use $\kappa_+^{1/2}$ as has been proposed in [21]. See also [30].

5 Experiments

We will now give a few numerical experiments to illustrate our methods. The implementations we have used are based on the level set evolution methods developed by Osher-Sethian [23, 24, 26, 27, 28], and the techniques in [19].

The equations described in this paper have been coded for the case of active contours on two-dimensional images. We will present here some experimental results obtained by running this code on both binary (i.e., high contrast images) and real images. Here the images have been selected purely for the purposes of illustration.

5.1 Numerical Aspects of Level Set Evolution

For 2D active contours, the evolution equation as derived in Section 3 is equation (8),

$$\frac{\partial \Psi}{\partial t} = \phi\|\nabla\Psi\|(\text{div}(\frac{\nabla\Psi}{\|\nabla\Psi\|}) + \nu) - \nabla\phi\cdot\nabla\Psi,$$

where ν is a constant inflation force and $\kappa := \text{div}(\frac{\nabla\Psi}{\|\nabla\Psi\|})$ is the curvature of the level sets of $\Psi(x,y,t)$. It is known that a propagating front may not remain smooth at all times (for example, it may cross itself). For evolution beyond the discontinuities the solutions are required to satisfy an entropy condition to ensure that the front remains physically meaningful at all times. Osher-Sethian [24] have given such entropy satisfying schemes and these have been used successfully in shape modelling [19]. Following [19] we can regard a decomposition of our speed function as,

$$F(\kappa) = \nu + \text{div}(\frac{\nabla\Psi}{\|\nabla\Psi\|}) = \nu + \kappa, \tag{14}$$

where ν is regarded as the constant passive advection term and the curvature κ is the diffusive term of the speed function. The inflation part in equation (8), i.e., $\nu\phi\|\nabla\Psi\|$ is approximated using upwind schemes. The diffusive part, i.e., $\kappa\phi\|\nabla\Psi\|$ is approximated using usual central differences. For the inner product term $\nabla\phi\cdot\nabla\Psi$, we use a certain thresholding smoothing method for the "doublet" $\nabla\phi$ which will be described in full detail in the journal version of this paper.

5.2 Image Feature Extraction Results

First we present the result of feature extraction on a synthetic high contrast image consisting of three shapes. The image is a 150 x 150 binary image with intensity values 0 or 255. Figure 2(a) shows the image with the initial contour. The time step used was $\Delta t = 0.000001$ and Figures 2(b) through 2(d) show the evolving contour at intermediate time steps. Figure 2(d) corresponds to 400 iterations. The value of the inflation force used was $\nu = 1600.0$.

In Figure 1 we present a convoluted shape to be extracted using an active contour. Figures 1(b) through 1(f) show the evolving contour at 200, 400, 600, 800, and 1000 iterations. The shape of the feature has been complelely captured by 1000 iterations. The value of the inflation force used in this example was $\nu = 100.0$.

The aim of the last experiment was to demonstrate the ability of the active contour in capturing the finer features in real images. The image is a 256 x 240 gray-scale image of a Rubik's cube placed on a circular table with a pattern on the table's side. An initial contour is placed with the aim of capturing the cube, the edge of the table and also the patterns on the side of the table. Figure 3(a) shows the intial contour. Figures 3(b) through 3(d) show the evolving contour after 100, 200, and 300 iterations. The time step used was $\Delta t = 0.001$. The inflationary force used was $\nu = 500.0$. At 300 iterations most of the patterns we wished to capture on the table's side have been captured. Notice that because of the initial configuration of the contour the edge of the table is captured from both inside and outside.

6 Conclusions

In this note, we have considered possible modifications of the active contour models based on those of [5, 19]. The basic concept is that we consider snakes in the framework of gradient flows relative to modified arc-length functionals. The active contour therefore flows to the desired feature regarded as lying at the bottom of the corresponding potential energy well. Possible 3-D surface models were also proposed using these energy ideas.

References

[1] L. Alvarez, F. Guichard, P. L. Lions, and J. M. Morel, "Axiomes et equations fondamentales du

traitement d'images," *C. R. Acad. Sci. Paris*, 315:135–138, 1992.

[2] L. Alvarez, P. L. Lions, and J. M. Morel, "Image selective smoothing and edge detection by nonlinear diffusion," *SIAM J. Numer. Anal.* **29**, pp. 845-866, 1992.

[3] A. Blake and A. Yuille, *Active Vision*, MIT Press, Cambridge, Mass., 1992.

[4] K. A. Brakke, *The Motion of a Surface by its Mean Curvature*, "Princeton University Press, Princeton, NJ, 1978.

[5] V. Caselles, F. Catte, T. Coll, and F. Dibos, "A geometric model for active contours in image processing," Technical Report #9210, CEREMADE, Université Paris Dauphine, 1992.

[6] V. Caselles and C. Sbert, "What is the best causal scale-space for 3D images?," Technical Report, Department of Math. and Comp. Sciences, University of Illes Balears, 07071 Palma de Mallorca, Spain, March 1994.

[7] M. P. Do Carmo, *Differential Geometry of Curves and Surfaces*, Prentice-Hall, Inc., New Jersey, 1976.

[8] C. L. Epstein and M. Gage, "The curve shortening flow," in *Wave Motion: Theory, Modeling, and Computation*, A. Chorin and A. Majda, Editors, Springer-Verlag, New York, 1987.

[9] M. Gage, "Curve shortening makes convex curves circular," *Invent. Math.* **76**, pp. 357-364, 1984.

[10] M. Gage and R. S. Hamilton, "The heat equation shrinking convex plane curves," *J. Differential Geometry* **23**, pp. 69-96, 1986.

[11] C. Gerhardt, "Flow of nonconvex hypersurfaces into spheres," *J. Differential Geometry* **32**, pp. 299-314, 1990.

[12] M. Grayson, "A short note on the evolution of a surface by its mean curvature," *Duke Math. Journal* **58**, pp. 555-558, 1989.

[13] M. Grayson, "The heat equation shrinks embedded plane curves to round points," *J. Differential Geometry* **26**, pp. 285-314, 1987.

[14] G. Huisken, "Flow by mean curvature of convex surfaces into spheres," *J. Differential Geometry* **20**, pp. 237-266, 1984.

[15] B. B. Kimia, A. Tannenbaum, and S. W. Zucker, "Toward a computational theory of shape: An overview", *Lecture Notes in Computer Science* **427**, pp. 402-407, Springer-Verlag, New York, 1990.

[16] B. B. Kimia, A. Tannenbaum, and S. W. Zucker, "Shapes, shocks, and deformations, I," to appear in *Int. J. Computer Vision.*

[17] A. Kumar, *Visual Information in a Feedback Loop*, Ph. D. thesis, University of Minnesota, 1995.

[18] A. Kumar, P. Olver, G. Sapiro, and A. Tannenbaum, "On an affine invariant active contour model," in preparation.

[19] R. Malladi, J. Sethian, and B. Vemuri, *Shape modeling with front propagation: a level set approach,* to appear in *IEEE Trans. Pattern Anal. Machine Intell.*

[20] F. Morgan, *Riemannian Geometry*, John and Bartlett Publishers, Boston, 1993.

[21] P. Neskovic and B. Kimia, "Three-dimensional shape representation from curvature-dependent deformations," Technical Report #128, LEMS, Brown University, 1994.

[22] P. Olver, G. Sapiro, and A. Tannenbaum, "Geomtric invariant evolution of surfaces and volumetric smoothing," submitted for publication in *SIAM J. Math. Anal.*, 1994.

[23] S. Osher, "Riemann solvers, the entropy condition, and difference approximations," *SIAM J. Numer. Anal.* **21**, pp. 217-235, 1984.

[24] S. J. Osher and J. A. Sethian, "Fronts propagation with curvature dependent speed: Algorithms based on Hamilton-Jacobi formulations," *Journal of Computational Physics* **79**, pp. 12-49, 1988.

[25] S. Osher and L. I. Rudin, "Feature-oriented image enhancement using shock filters," *SIAM J. Numer. Anal.* **27**, pp. 919-940, 1990.

[26] J. A. Sethian, *An Analysis of Flame Propagation*, Ph. D. Dissertation, University of California, 1982.

[27] J. A. Sethian, "Curvature and the evolution of fronts," *Commun. Math. Phys.* **101**, pp. 487-499, 1985

[28] J. A. Sethian, "A review of recent numerical algorithms for hypersurfaces moving with curvature dependent speed," *J. Differential Geometry* **31**, pp. 131-161, 1989.

[29] J. A. Sethian and J. Strain, "Crystal growth and dendritic solidification," *Journal of Computational Physics* **98**, 1992.

[30] H. Tek and B. Kimia, "Deformable bubbles in the reaction-diffusion space," Technical Report #138, LEMS, Brown University, 1994.

[31] B. White, "Some recent developments in differential geometry," *Mathematical Intelligencer* **11**, pp. 41-47, 1989.

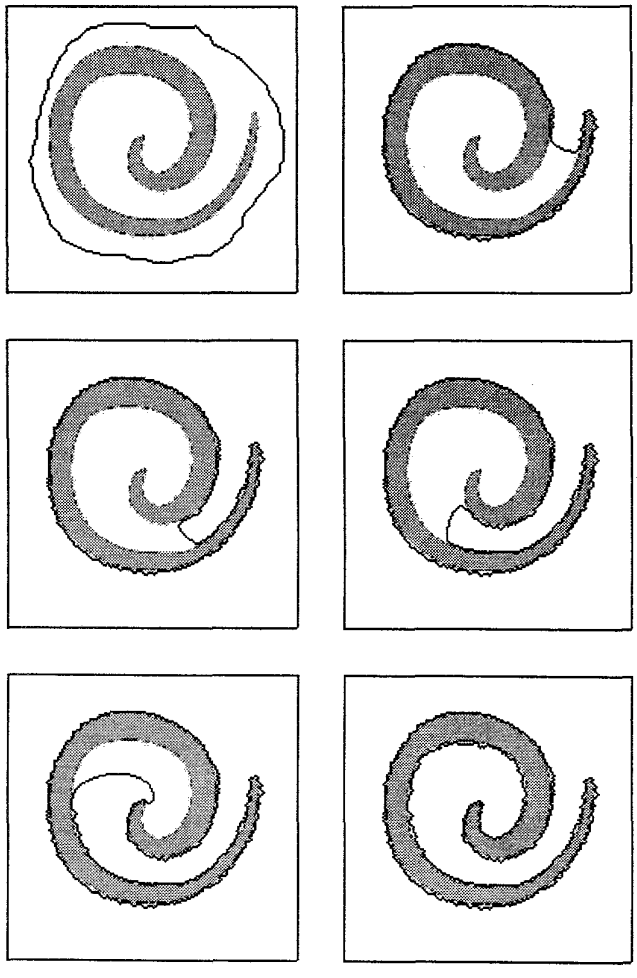

Figure 1: Feature extraction in a synthetic image. Left to right, top to bottom: (a) Initial contour. (b),(c),(d),(e),and (f) contour after 200, 400, 600, 800 and 1000 iterations. $\Delta t = 0.000001$.

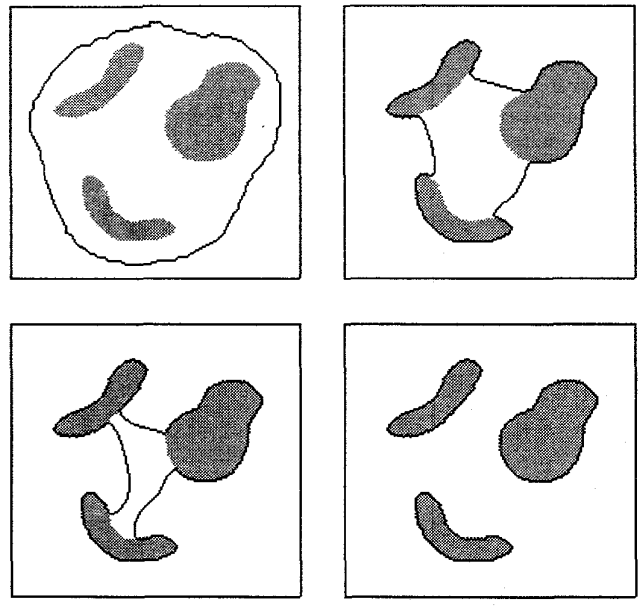

Figure 2: Feature extraction in a synthetic image. Left to right, top to bottom: (a) Initial contour. (b),(c),and (d) contour after 200, 300, and 400 iterations. $\Delta t = 0.000001$.

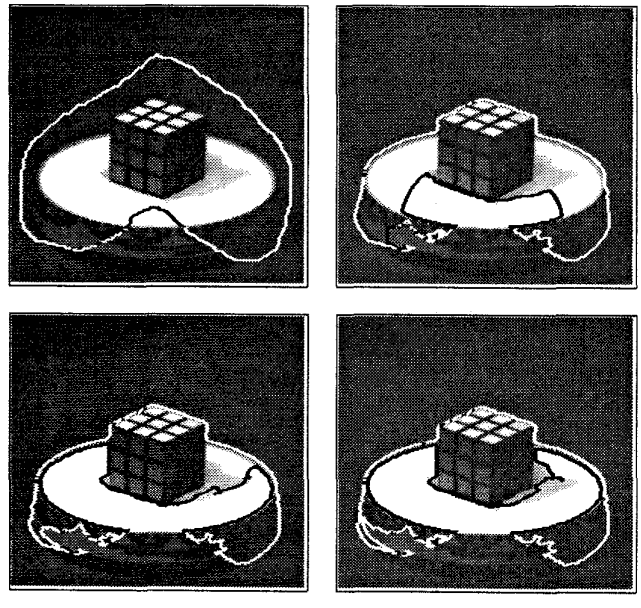

Figure 3: Feature extraction in a real image. Left to right, top to bottom: (a) Initial contour. (b),(c),and (d) contour after 100, 200, and 300 iterations. $\Delta t = 0.001$.